Weak universality of spin-glass transitions in three-dimensional $\pm J$ models

2003 J. Phys. A: Math. Gen. 36 10895

(http://iopscience.iop.org/0305-4470/36/43/015)

INSTITUTE OF PHYSICS PUBLISHING JOURNAL OF PHYSICS A: MATHEMATICAL AND GENERAL

J. Phys. A: Math. Gen. **36** (2003) 10895–10906 PII: S0305-4470(03)63090-8

Weak universality of spin-glass transitions in three-dimensional $\pm J$ models

Tota Nakamura, Shin-ichi Endoh[1] and Takeo Yamamoto

Department of Applied Physics, Tohoku University, Aoba-yama 05, Sendai, Miyagi 980-8579, Japan

Received 1 May 2003, in final form 29 July 2003
Published 15 October 2003
Online at stacks.iop.org/JPhysA/36/10895

Abstract

We find the possibility of weak universality of spin-glass phase transitions in three-dimensional $\pm J$ models. The Ising, the XY and the Heisenberg models seem to undergo finite-temperature phase transitions with a ratio of the critical exponents $\gamma/\nu \sim 2.4$. Evaluated critical exponents may explain the corresponding experimental results. The analyses are based upon nonequilibrium relaxation from a paramagnetic state and finite-time scaling.

PACS numbers: 75.10.Nr, 64.60.−i

1. Introduction

The spin-glass (SG) phenomenon has been attracting great interest both theoretically and experimentally [1]. Applications now cover a wide range of interdisciplinary fields of statistical physics and informational physics, as treated in this special issue. However, many subjects are not well understood, in spite of efforts made over almost 30 years. One of these subjects is whether or not the SG transition of real materials can be explained by a simple random-bond spin model.

Spins of many SG materials are well approximated by the Heisenberg spins. The simplest theoretical model is the Heisenberg model with random nearest-neighbour interactions. However, numerical studies suggest that there is no finite-temperature SG transition in this model [2, 3]. Kawamura [4, 5] proposed the chirality mechanism in order to solve this discrepancy. The chiral-glass (CG) transition occurs without the SG order. A small but finite random anisotropy in the real materials mixes the chirality degrees of freedom and the spin degrees of freedom. This anisotropy effect induces the SG transition observed in the real materials. The scenario is based upon results that the SG transition does not occur in the isotropic model. However, Matsubara *et al* [6–8] recalculated the domain-wall excess energy and the SG susceptibility, from which they suggested that the finite-temperature SG transition

[1] Present address: Birds Systems Research Institute Inc., 1-6-15 Hirakawa-cho, Chiyoda-ku, Tokyo 102-0093, Japan.

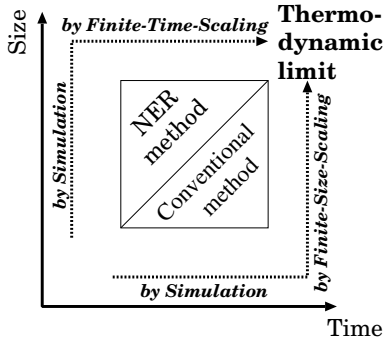

Figure 1. A schematic diagram to approach the thermodynamic limit.

does possibly occur. Methods are quite similar to the previous ones [2, 3]. Subtle differences in the analyses of the obtained data drew opposite conclusions.

The spin-glass problem is one of the most difficult subjects in computational physics. It can be a tough bench-mark test for a new numerical method. It may be applied to other complex systems, if successful in the spin-glass investigations. The difficulty is caused by serious slow dynamics. It requires many Monte Carlo steps to reach the equilibrium states. An observed quantity at each step has a strong correlation even after the equilibration. The system sizes which can be treated in the simulations are accordingly limited to very small ones, e.g., mostly of linear size 20 or less in three dimensions. Size effects are generally stronger in the continuous spin systems because the spins are soft and the boundary effect propagates faster. Frustration and randomness also yield a considerable size effect. The system sizes treated previously in the studies of the Heisenberg SG models are too small to extrapolate to the thermodynamic limit. This is our motivation for reexamining the SG transition using the nonequilibrium relaxation (NER) method [9–14].

The difficulty mentioned above can be overcome by using the NER method. This method takes the opposite approach to the thermodynamic limit. Figure 1 schematically shows a comparison between the conventional equilibrium simulational method and the NER method. In the conventional method one takes the infinite time limit first by achieving the equilibrium states at finite sizes. The thermodynamic limit is taken by the finite-size scaling analysis of the obtained data. In the NER method we take the infinite-size limit first by dealing with a very large system within a finite time range before the finite-size effect appears. Then, the *finite-time scaling analysis* [15, 16] is performed to obtain the thermodynamic properties. The cost of a simulation is of the same order of L^{d+z} for both methods. However, the coefficient factor in the NER method is much smaller than that in the conventional method. An observation time length in the NER method is sufficient if we can observe the beginning of a final relaxation to the equilibrium states (equilibrium relaxation). On the other hand, it is necessary to wait until the end of the equilibrium relaxation in the conventional method. The latter time scale is typically 10–10^2 times longer than the former one in the spin-glass models. (For example, $\chi_{\rm sg}$ of $L = 17$ in figure 4(a) or $\chi_{\rm sg}$ at $T = 0.56$ in figure 6(a).) Therefore, the NER method has an advantage over the conventional method by this factor. We use the residual computational time to enlarge the system size and to increase statistical accuracy.

By using the NER method we have made it clear that the SG transition occurs in the Heisenberg model at the same finite temperature as the CG transition occurs [17]. The estimated critical exponent γ is consistent with the corresponding experimental result [18].

The chirality mechanism is not necessary to explain the spin-glass experiments since the chirality trivially freezes if the spin freezes. However, one may question the use and the validity of the NER method in the spin-glass phenomenon. Therefore, we have corroborated our method by studying the Ising SG model. Many numerical investigations [19–23] yield consistent results on the existence of the SG transition, the critical temperature and the critical exponents. They are also consistent with the corresponding experimental results [24]. The NER method yields consistent results for a small number of simulations as discussed in section 3.

In this procedure we have found a possibility of a weak universality: a critical exponent divided by ν, for example γ/ν, is common among models in a weak universality class. The ratio of the critical exponents $\gamma/z\nu$ appearing in finite-time scaling analysis is found to be consistent between the Heisenberg model and the Ising model. We have verified that a ratio γ/ν is also consistent by evaluating the dynamic exponent z alone. The analysis is expanded to the XY SG model and the value is also found to be consistent. These findings are quite surprising. We must reconsider the role of the spin dimensions and the distribution of the randomness in the SG phase transition.

This paper is organized as follows. In section 2 the model and the method are explained. Descriptions of the procedure of the NER method and the finite-time scaling are given. In section 3 the results on the Ising model, the Heisenberg model and the XY model are shown. Then, the possibility of a weak universality is discussed. Section 4 is devoted to a summary.

2. Model and method—nonequilibrium relaxation

The model treated in this paper is the nearest-neighbour $\pm J$ random-bond model,

$$\mathcal{H} = \sum_{\langle i,j\rangle} J_{ij}\boldsymbol{S}_i \cdot \boldsymbol{S}_j. \tag{1}$$

The linear size of a lattice is denoted by L. Skewed periodic boundary conditions are imposed, i.e. total numbers of spins $N = L \times L \times (L+1)$. An interaction J_{ij} takes two values of $+J$ and $-J$ with the same probability. The temperature T is scaled by J.

Spins are updated by a single-spin-flip algorithm. The Metropolis (M) update is used in all models, whereas the heat-bath (H) update [3] is used in the Heisenberg model. Physical quantities observed in our simulations are the SG susceptibility $\chi_{\rm sg}$, the CG susceptibility $\chi_{\rm cg}$ and the Binder parameter with regard to the spin-glass transition $g_{\rm sg}$. These quantities are calculated through the overlap between real replicas.

First, we rewrite the thermal average by an arithmetic mean over thermally equilibrium ensembles labelled by α as

$$\langle \boldsymbol{S}_i \cdot \boldsymbol{S}_j\rangle = \frac{1}{m}\sum_{\alpha=1}^{m} \boldsymbol{S}_i^{(\alpha)} \cdot \boldsymbol{S}_j^{(\alpha)} = \frac{1}{m}\sum_{\alpha=1}^{m}\sum_{\mu}^{x,y,z} S_{i,\mu}^{(\alpha)} S_{j,\mu}^{(\alpha)}. \tag{2}$$

The bracket $\langle\cdots\rangle$ denotes the thermal average and m denotes the number of ensembles. The index μ stands for three components of spins: x, y and z. This expression is substituted into the definition of the SG susceptibility:

$$\chi_{\rm sg} = \frac{1}{N}\sum_{i,j}[\langle \boldsymbol{S}_i \cdot \boldsymbol{S}_j\rangle^2]_{\rm c} = N\left[\frac{1}{m^2}\sum_{\alpha,\beta}^{m}\sum_{\mu,\nu}^{x,y,z}\left(q_{\mu,\nu}^{\alpha\beta}\right)^2\right]_{\rm c} \tag{3}$$

where $q_{\mu,\nu}^{\alpha\beta} \equiv (1/N)\sum_i S_{i,\mu}^{(\alpha)} S_{i,\nu}^{(\beta)}$ is an overlap between the μ component of a spin i on an ensemble α: $S_{i,\mu}^{(\alpha)}$ and the ν component of the spin on an ensemble β: $S_{i,\nu}^{(\beta)}$. The bracket $[\cdots]_{\rm c}$ denotes the configurational average.

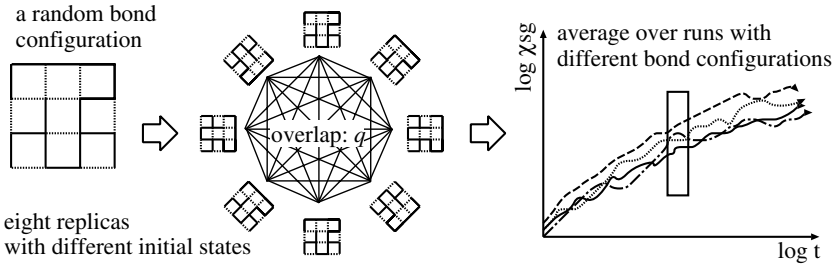

Figure 2. A schematic flow diagram of our simulation. Solid bonds and broken bonds in the lattice depict ferromagnetic bonds and antiferromagnetic bonds.

Here, we introduce the following real replicas. Each real replica takes the same random bond configuration and the different paramagnetic initial spin state. They are updated in parallel with different random number sequences. This procedure corresponds to quenching from an infinite temperature. The thermal ensembles are realized by these real replicas which approach different equilibrium states. Therefore, we replace the thermal average by the average over these real replicas as equation (2). The indices α and β now represent real replicas. We do not take into consideration a constant term which arises from the overlap between the same replica $\alpha = \beta$ and use the following expressions in the simulations:

$$\chi_{\mathrm{sg}} = N\left[\frac{2}{m(m-1)}\sum_{\alpha>\beta}^{m}\sum_{\mu,\nu}^{x,y,z}\left(q_{\mu,\nu}^{\alpha\beta}\right)^2\right]_{\mathrm{c}} \tag{4}$$

$$\chi_{\mathrm{cg}} = \frac{1}{3N}\left[\frac{2}{m(m-1)}\sum_{\alpha>\beta}^{m}\left(\sum_{i,\phi} C_{i,\phi}^{(\alpha)} C_{i,\phi}^{(\beta)}\right)^2\right]_{\mathrm{c}} \tag{5}$$

$$g_{\mathrm{sg}} = \frac{1}{2}\left(A - B\frac{\sum_{\mu,\nu,\delta,\rho}\left[\frac{2}{m(m-1)}\sum_{\alpha>\beta}^{m}\left(q_{\mu,\nu}^{\alpha\beta}\right)^2\left(q_{\delta,\rho}^{\alpha\beta}\right)^2\right]_{\mathrm{c}}}{\left(\sum_{\mu,\nu}\left[\frac{2}{m(m-1)}\sum_{\alpha>\beta}^{m}\left(q_{\mu,\nu}^{\alpha\beta}\right)^2\right]_{\mathrm{c}}\right)^2}\right). \tag{6}$$

The number of replicas m controls the precision of the thermal average. It is better to take a large value. We prepare eight or nine replicas for each bond configuration in this paper. The scalar chirality is defined by three neighbouring spins as $C_{i,\phi}^{(\alpha)} = \boldsymbol{S}_{i+\hat{e}_\phi}^{(\alpha)} \cdot \left(\boldsymbol{S}_i^{(\alpha)} \times \boldsymbol{S}_{i-\hat{e}_\phi}^{(\alpha)}\right)$, where $\hat{e}_\phi$ denotes a unit lattice vector along the ϕ axis. In the XY model we calculate the vector chirality, which is defined by $C_{i,\phi}^{(\alpha)} = (1/2\sqrt{2})\left(J_{ij}\boldsymbol{S}_i^{(\alpha)} \times \boldsymbol{S}_j^{(\alpha)} + J_{jk}\boldsymbol{S}_j^{(\alpha)} \times \boldsymbol{S}_k^{(\alpha)} + J_{kl}\boldsymbol{S}_k^{(\alpha)} \times \boldsymbol{S}_l^{(\alpha)} + J_{li}\boldsymbol{S}_l^{(\alpha)} \times \boldsymbol{S}_i^{(\alpha)}\right)\big|_z$. Indices i, j, k, l denote four sites forming a square plaquette in the ϕ direction from the i site. Constants in a definition of g_{sg} are $A = 3$, $B = 1$ for the Ising model, $A = 6$, $B = 4$ for the XY model and $A = 11$, $B = 9$ for the Heisenberg model.

Figure 2 shows a schematic diagram of the simulation procedure. We calculate a physical quantity at each time step t and obtain a relaxation function. Another simulation starts by changing a random bond configuration, initial spin states and a random number sequence. Then, another relaxation function is obtained. Finally, we take an average of data at each step over these different Monte Carlo runs. It should be noted that the average is over independent data. It guarantees the absence of systematic error due to correlations of the observed quantity, which we usually encounter in the conventional Monte Carlo time average. The obtained raw relaxation function is utilized by the following finite-time scaling analysis.

Table 1. Numbers of bond configurations to obtain data for χ_{sg} and g_{sg} at T_{sg} in this paper. Indices (M) and (H) in the Heisenberg model denote update algorithms: (M) for the Metropolis and (H) for the heat bath. Arrows mean that the number is same as to the right.

			Step						
	Model	Size	10^3	10^4	5×10^4	10^5	5×10^5	10^6	4×10^6
χ_{sg}	Ising	49	→	→	→	393	→	→	88
	XY	39	→	→	→	5246	120		
	Heisenberg(M)	59	→	→	→	→	→	104	
	Heisenberg(H)	89	→	58	→	22			
g_{sg}	Ising	39	255480	85480	18576	12626	→	1830	172
	XY	19	→	→	→	7803			
	Heisenberg(H)	39	43114	18316	7038				

The most important point in the NER method is to exclude finite-size effects from the raw relaxation function. The method is based upon taking the infinite-size limit first. If a relaxation function includes a finite-size effect, it exhibits converging behaviour because every finite system has a definite equilibrium state. This behaviour misleads us into thinking that the temperature is in the paramagnetic phase even though it is the critical temperature. Therefore, the critical temperature is always underestimated if the size is insufficient. We check the size effect by changing the lattice sizes and always confirm a time range in which the size can be considered as infinity.

The SG susceptibility is expected to diverge at the critical temperature (T_{sg}) as $\chi_{sg}(t) \sim t^{\gamma/z\nu}$ [13]. We obtain T_{sg}, γ and $z\nu$ by the finite-time scaling analysis on the relaxation functions of $\chi_{sg}(t)$ in the paramagnetic phase [17]. Since the initial spin configuration is completely random, $\chi_{sg}(t = 0) \sim 1$. We start a set of simulations at a temperature T that is obviously in the paramagnetic phase. The relaxation function $\chi_{sg}(t)$ at this temperature increases with t but soon converges to a finite value. As the temperature is lowered to approach the critical temperature, the relaxation function tends to show diverging behaviour. Since the temperature is still in the paramagnetic phase, the relaxation finally converges to a finite value after a correlation time $\tau(T)$. The spin-glass correlation increases with time and reaches the correlation length $\xi(T)$ after this correlation time. Two quantities relate to each other by z as $\tau(T) \sim \xi^z(T)$. Therefore, the correlation time should diverge at T_{sg} as

$$\tau(T) \sim (T - T_{sg})^{-z\nu}. \tag{7}$$

The correlation time can be estimated by scaling the raw relaxation function. We obtain $\gamma/z\nu$ and $\tau(T)$ so that the scaled functions $\chi_{sg}(t)t^{-\gamma/z\nu}$ at all temperatures plotted against $t/\tau(T)$ fall onto a single curve. Then, the critical temperature and the exponent $z\nu$ are estimated by the least-squares fitting with equation (7). Since a ratio $\gamma/z\nu$ is already estimated by the scaling, γ is obtained.

The NER of the Binder parameter $g_{sg}(t)$ is calculated at the obtained T_{sg}. Since quantity is related to the fourth-order cumulant, many bond samples are necessary to obtain meaningful data. The number of bond configurations to obtain the results in this paper is summarized in table 1. The Binder parameter is expected to diverge at T_{sg} as $g_{sg}(t) \times L^d \sim t^{d/z}$ [14], by which z is independently obtained. Then, ν is estimated from a value of $z\nu$ obtained by the τ-fitting explained above. All exponents are now estimated by the scaling relation. It is possible to compare the critical exponents with the experimental results.

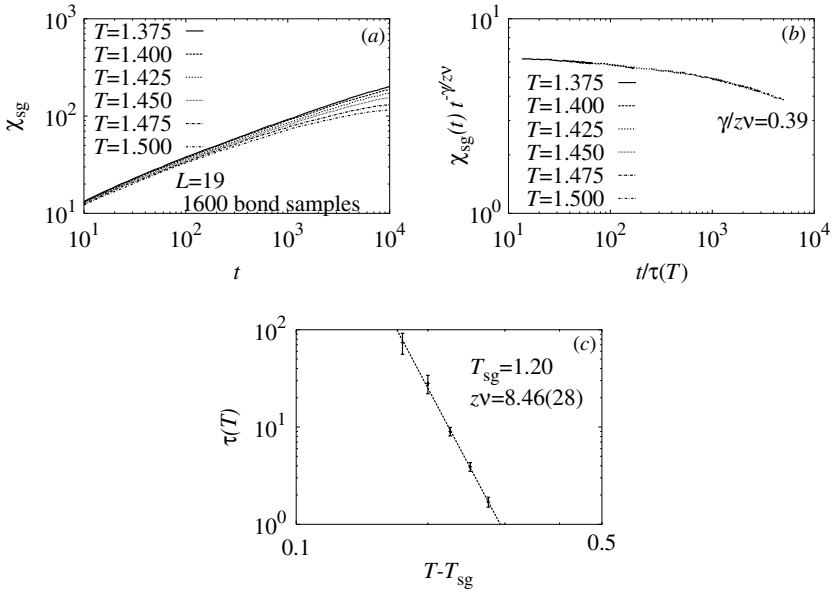

Figure 3. (*a*) The NER of χ_{sg} of the Ising model at high temperatures. (*b*) The finite-time scaling plot for a choice of $\gamma/z\nu = 0.39$. We obtain $\tau(T)$ and $\gamma/z\nu$ so that this scaling plot is good. The scaling is also possible for $\gamma/z\nu = 0.38$–0.40. (*c*) The least-squares fitting of $\tau(T)$ supposing $\tau(T) \propto |T - T_{sg}|^{-z\nu}$.

The last procedure of our method is to corroborate the results by observing the NER of χ_{sg} at the obtained T_{sg}. It should diverge as $t^{\gamma/z\nu}$ with the same exponent as obtained by finite-time scaling. If the exponents are inconsistent, the scaling analysis is misled by an insufficient time range or by the finite-size effect. In the Ising model we perform another check at T_{sg} by observing the NER of the distribution function of the replica overlap, $P(q, t)$. The finite-time scaling plot of $P(q, t)$ should ride on a single scaling function with the same exponent obtained by finite-time scaling of χ_{sg}. This is a direct interpretation of the finite-size scaling of $P(q, L)$ [20] by $t \propto L^z$.

3. Results

Numbers of bond configurations to obtain data at the critical temperature are summarized in table 1. The numbers at other temperatures are mostly of the same order. For each bond configuration, we prepared eight replicas for the XY and the Heisenberg model and nine replicas for the Ising model.

3.1. Ising model

Figure 3 shows an analysis to determine the critical temperature and the exponent. The simulation is performed just to check that our method gives results consistent with previous investigations [19–23]. Therefore, the system size is very small ($L = 19$) and the time range is very short. Finite-size effects are found to appear for $t > 5000$ by comparing with results for $L = 29$. Only data before this time are used in the scaling analysis. Figure 3(*b*) is an example of finite-time scaling. A choice of $\gamma/z\nu$ is possible for $\gamma/z\nu = 0.38$–0.40. A set

Table 2. A list of the critical temperatures and exponents $z\nu$ obtained by the finite-time scaling analysis in the Ising model. The ratio of exponents $\gamma/z\nu$ denotes the possible value in the finite-time scaling. The least-squares fitting errors are denoted by χ^2.

$\gamma/z\nu$	$T_{\rm sg}$	$z\nu$	γ	χ^2
0.400	1.05	12.63(18)	5.1(1)	1.40
0.395	1.13	10.07(37)	4.0(2)	0.66
0.390	1.20	8.46(28)	3.3(1)	0.54
0.385	1.22	8.67(9)	3.3(0)	1.49
0.380	1.21	9.82(9)	3.7(0)	1.84

of correlation times at each temperature is estimated for each choice of this exponent. Then, the critical temperature is obtained as summarized in table 2. As the exponent increases, $T_{\rm sg}$ decreases. We ignore a result of $\gamma/z\nu = 0.400$ which deviates a lot from the others. Our estimates are

$$T_{\rm sg} = 1.17(4) \qquad \gamma/z\nu = 0.3875(75) \qquad z\nu = 9.3(12) \qquad \gamma = 3.7(5). \tag{8}$$

The results of the finite-time scaling analysis are checked by the raw NER data at the obtained critical temperature. Figure 4(*a*) shows relaxation data of $\chi_{\rm sg}$ and $g_{\rm sg} \times L^d$. The SG susceptibility diverges algebraically with an exponent $\gamma/z\nu = 0.38$ that is consistent with the scaling result $\gamma/z\nu = 0.3875(75)$. The critical relaxation process begins around $t \sim 100$ and seems to continue to infinity. The Binder parameter also shows diverging behaviour with $t^{d/z}$, from which we obtain the dynamic exponent $z = 6.2(2)$. Then, an exponent ν is estimated as $\nu = 1.5(3)$. The ratio of the critical exponents $\gamma/\nu = 2.4(1)$. The obtained results are consistent with previous numerical investigations [19–23] and the corresponding experimental results [24] as summarized in table 3. Since the lattice size and the time range are insufficient, the final numerical results have large error bars. As discussed in the previous section, the critical temperature may be underestimated by using a small lattice. We plan to estimate them with high accuracy by large scale NER analyses.

The time evolution of the distribution function of the overlap $P(q, t)$ at $T = T_{\rm sg} = 1.17$ is shown in figure 4(*b*). The system size $L = 17$. It exhibits a single Gaussian form with a peak at $q = 0$ before the size effect of $\chi_{\rm sg}$ appears at $t = 10^5$ as shown in figure 4(*a*). As time increases, the width of the distribution grows in accordance with the divergence of the spin-glass susceptibility. It is possible to scale $P(q, t)/t^{\gamma/2z\nu}$ plotted versus $qt^{\gamma/2z\nu}$ for various time steps from $t = 10$ to $t = 10^4$ (figure 4(*c*)). The critical exponent $\gamma/z\nu$ is also consistent with the finite-time scaling of $\chi_{\rm sg}$. The scaled data deviate a little for $t = 10$ because the time is just before the relaxation of $\chi_{\rm sg}$ reaches the critical relaxation region as shown in figure 4(*a*). The distribution changes its shape to having two peaks at $\pm q_{\rm eq}$ after the finite-size effect appears. The shape is flat at this crossover time.

It is found that the NER function knows the critical phenomenon from its very early time steps: $t = 10$–100. The NER method is now clearly shown to be applicable to the spin-glass phenomenon.

3.2. Heisenberg model

We apply the same analysis performed in the Ising model to the Heisenberg model. Finite-time scaling results have already been shown briefly in [17] and the detailed analysis will be reported elsewhere. The system size is $L = 59$ and the time scale is 70 000 Monte Carlo steps.

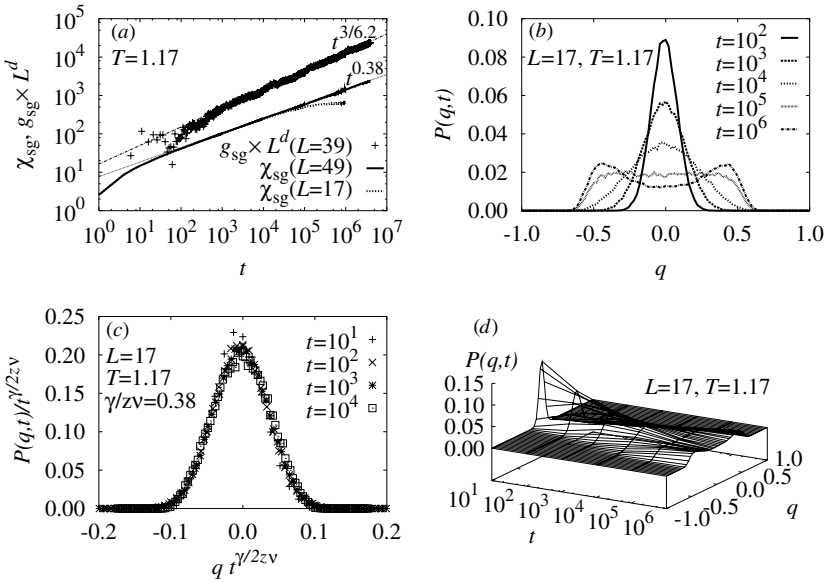

Figure 4. (*a*) The NER of $\chi_{\rm sg}$ and $g_{\rm sg} \times L^d$ of the Ising model at $T_{\rm sg} = 1.17$. Two lines, $t^{\gamma/z\nu}$ with $\gamma/z\nu = 0.38$ and $t^{d/z}$ with $z = 6.2$, are guides for the eyes. (*b*) The NER of the distribution function $P(q, t)$ at $T_{\rm sg}$ for $L = 17$. The shape changes from single peaked to double peaked when the size effect of $\chi_{\rm sg}$ appears at $t = 10^5$. (*c*) The finite-time scaling plot of $P(q, t)$. (*d*) A three-dimensional plot of $P(q, t)$.

Table 3. Estimates of $T_{\rm sg}$, γ, ν, γ/ν and z in the $\pm J$ models in three dimensions.

	$T_{\rm sg}$	γ	ν	γ/ν	z
Ising SG					
Present work	1.17(4)	3.6(6)	1.5(3)	2.4(1)	6.2(2)
Reference [21]	1.11(4)	4.0(8)	1.7(4)	2.35(5)	
Reference [23]	1.195(15)	2.95(30)	1.35(10)	2.225(25)	5.65(15)
Experiment [24]		4.0(3)	∼1.7	∼2.4	
Heisenberg SG					
Present work	0.20(2)	1.9(5)	0.8(2)	2.3(3)	6.2(5)
Reference [8]	0.18(1)	2.0(2)	0.97(5)	2.1(1)	
Experiment [18]		2.3(4)	1.25(25)	2.0(7)	
XY SG					
Present work	0.43(3)			2.4(2)	6.8(5)

Typical numbers of bond configurations are same as given in table 1. The finite-time scaling results are

$$T_{\rm sg} = 0.20(2) \qquad \gamma/z\nu = 0.39(5) \qquad z\nu = 4.8(10) \qquad \gamma = 1.9(5). \tag{9}$$

These results are checked by the raw NER at $T = 0.21$ as shown in figure 5. The SG susceptibility diverges algebraically with an exponent $\gamma/z\nu = 0.38$, which is consistent with the result of finite-time scaling. We performed simulations of both Metropolis update and heat-bath update. The Metropolis result denoted by (M) and the heat-bath result denoted by (H) exhibit the same critical behaviour, while the amplitudes are different by a factor of 3.5.

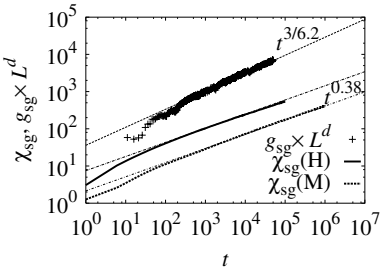

Figure 5. The NER of χ_{sg} and $g_{sg} \times L^d$ of the Heisenberg model at $T_{sg} = 0.21$. Lattice sizes are $L = 39$ for $g_{sg} \times L^d$, $L = 89$ for χ_{sg}(H) and $L = 59$ for χ_{sg}(M). Indices (H) and (M) denote the heat-bath update and the Metropolis update, respectively. Lines, $t^{\gamma/z\nu}$ with $\gamma/z\nu = 0.38$ and $t^{d/z}$ with $z = 6.2$, are guides for the eyes.

The NER behaviour is independent of the update algorithm. The consistency supports the criticality of the SG order at this temperature. It is noted that the critical divergence begins at a very early time: $t \sim 100$.

The Binder parameter exhibits a critical divergence $t^{d/z}$ with $z = 6.2(5)$. The value is consistent with that in the Ising model. Since $z\nu$ is obtained by finite-time scaling, ν is estimated as $\nu = 0.8(2)$. The ratio of the critical exponent $\gamma/\nu = 2.3(3)$. The results are compared with an experimental result [18] in table 3. They are not inconsistent.

3.3. XY model

It has been considered that there is no SG transition in this model [25, 26]. Only the CG transition with respect to the vector chirality is considered to occur [27–29]. However, the possibility of a SG transition has recently been identified by several investigations [30–32]. We applied the NER analysis to this model and our result supports the latter conclusion: the SG transition occurs.

Our finite-time scaling analysis on the XY model is not yet conclusive with regard to whether the SG transition and the CG transition occur at the same temperature or not. The system size ($L = 39$), Monte Carlo steps (10^5) and the temperature range used in the scaling analysis are insufficient to extract a conclusion. However, as we increase the size and the number of steps, both critical temperatures seem to approach each other: T_{sg} increases from low and T_{cg} decreases from high. Therefore, we consider that both transitions occur simultaneously. Investigations are now being carried out and the details will be reported elsewhere. What has now been made clear is that both transitions occur in a temperature range of $0.4 < T < 0.46$. In this paper we do not examine the issue of simultaneous transition but focus on the existence of the SG transition.

Figure 6(*a*) shows raw NER plots of χ_{sg} and χ_{cg} near and above the critical temperature. There is no difference in χ_{sg} between $T = 0.43$ and $T = 0.46$ within the present time steps. They exhibit a critical divergence with the same exponent and amplitude. The SG transition is considered to occur near $T = 0.43$. From the slope we obtain an exponent $\gamma/z\nu = 0.35$. Note that this value is a little smaller than that of the Ising model and the Heisenberg model ($\gamma/z\nu \sim 0.38$). The NER of the Binder parameter is shown in figure 6(*b*). It exhibits a critical divergence with an exponent d/z with $z = 6.8(5)$, which is also a little larger than that of the other models. However, we obtain the ratio of the critical exponents $\gamma/\nu = 2.4(2)$, which is consistent with the other models.

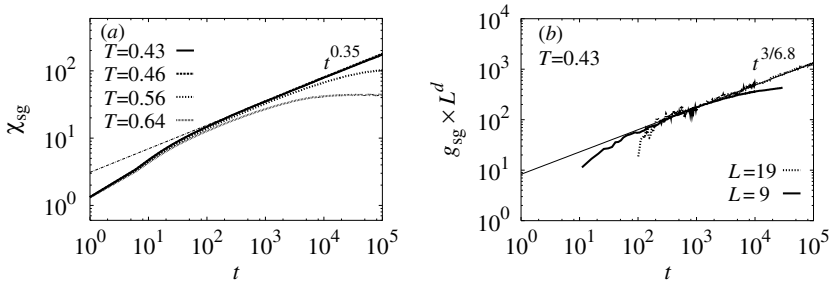

Figure 6. (*a*) The NER of χ_{sg} in the XY model above the critical temperature $T_{sg} \sim 0.43$. Lattice size is $L = 39$. The line $t^{\gamma/z\nu}$ with $\gamma/z\nu = 0.35$ is a guide for the eyes. (*b*) The NER of the Binder parameter multiplied by L^d. The line $t^{d/z}$ with $z = 6.8$ is a guide for the eyes.

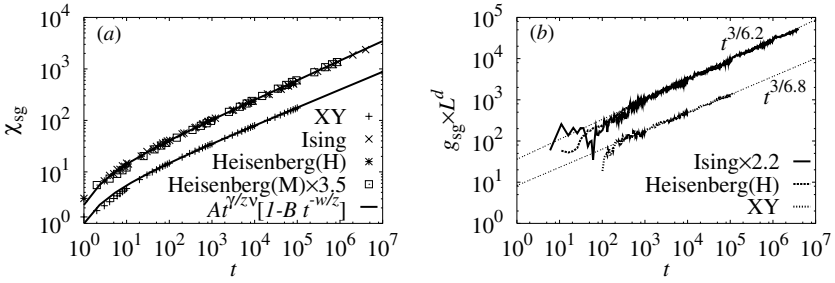

Figure 7. (*a*) NER plots of the χ_{sg} at T_{sg}. Correction-to-scaling fittings are depicted by bold lines with $\gamma/\nu = 2.356$, $w = 3$, $z = 6.2$ for the Ising/Heisenberg model and $z = 6.8$ for the XY model. NER functions except the XY model are indistinguishable. The data of the Heisenberg model with the Metropolis update are multiplied by 3.5. (*b*) NER plots of the Binder parameter multiplied by L^d. The relaxation function of the Ising model multiplied by 2.2 coincides with that of the Heisenberg model with the heat-bath update.

3.4. Weak universality

The SG transition occurs in all models as shown in the preceding subsections. The ratio of the critical exponents γ/ν takes a common value around 2.4. Therefore, there is a possibility of weak universality among these transitions. Not only the value of γ/ν but also the NER functions themselves suggest that the transitions are qualitatively equivalent.

Figure 7(*a*) shows the NER functions of χ_{sg} at the critical temperature for all the models treated in this paper. The data of the Heisenberg model with the Metropolis update are multiplied by a factor 3.5 in order to compare with the result of the Ising model and that of the Heisenberg model with the heat-bath update. These three NER functions are not distinguishable. If we take into account a correction-to-scaling term, the relaxation functions can be fitted from the first few steps (bold lines in figure 7(*a*)) by an expression [23]:

$$At^{\gamma/z\nu}[1 - Bt^{-w/z}]. \tag{10}$$

Here, the exponents of the leading term are set $\gamma/\nu = 2.356$ and $z = 6.2$. The correction-to-scaling exponent $w = 3$. Coefficient constants are $A = 7.6$ and $B = 0.7$. The same expression also fits the NER function of the XY model, but with the dynamic exponent $z = 6.8$ and a constant $A = 3.3$. The NER functions of the Binder parameter are shown in figure 7(*b*). If we multiply the result of the Ising model by a factor 2.2, it is indistinguishable from the curve of the Heisenberg model.

4. Summary

By applying the nonequilibrium relaxation method it has been made clear that the $\pm J$ models in three dimensions undergo finite-temperature spin-glass transitions. There is a possibility that these models belong to the same weak universality class with the ratio of the critical exponents $\gamma/\nu \sim 2.4$. We compare our results with other numerical results and the experimental results in table 3. They agree well within the numerical errors. Since the error bars are rather large at present, further efforts to improve precision are necessary in order to prove weak universality.

The spin-glass transition of the Heisenberg model is found to be very similar to that of the Ising model. The relaxation functions of $\chi_{\rm sg}$ and $g_{\rm sg}$ and values of the ratio of the exponents γ/ν and the dynamic exponent z are consistent between the two models. If one considers that the spin-glass transition occurs in the Ising model, it may be thought that it occurs in the Heisenberg model to the same accuracy. Only the dynamic exponent of the XY model differs from the other models. Spin-glass transition and weak universality in models with Gaussian bond distributions is a problem to be checked in future work. The type of bond distribution may be important.

The NER method has been shown to be particularly effective in the spin-glass study. Critical behaviour is observed from very early time steps even though it takes a very long time to achieve the equilibrium states. What is long is the nonequilibrium relaxation process after a short initial relaxation before the final equilibrium relaxation. This long process is discarded in conventional simulations, while it is utilized in the NER method. This is one reason why the NER method is advantageous in this system. Applications to various complex systems with slow dynamics are fruitful [33, 34].

Acknowledgments

The authors would like to thank Professor Fumitaka Matsubara for guiding them in the spin-glass study and for their fruitful discussions. The author TN also thanks Professor Nobuyasu Ito and Professor Yasumasa Kanada for providing him with a fast random number generator RNDTIK. Computations were partly done at the Supercomputer Center, ISSP, The University of Tokyo.

References

[1] For a review see Binder K and Young A P 1986 *Rev. Mod. Phys.* **58** 801
Mydosh J A 1993 *Spin Glasses* (London: Taylor & Francis)
Young A P (ed) 1997 *Spin Glasses and Random Fields* (Singapore: World Scientific)
[2] McMillan W L 1985 *Phys. Rev.* B **31** 342
[3] Olive J A, Young A P and Sherrington D 1986 *Phys. Rev.* B **34** 6341
[4] Kawamura H 1992 *Phys. Rev. Lett.* **68** 3785
[5] Hukushima K and Kawamura H 2000 *Phys. Rev.* E **61** R1008
[6] Matsubara F, Endoh S and Shirakura T 2000 *J. Phys. Soc. Japan* **69** 1927
[7] Endoh S, Matsubara F and Shirakura T 2001 *J. Phys. Soc. Japan* **70** 1543
[8] Matsubara F, Shirakura T and Endoh S 2001 *Phys. Rev.* B **64** 092412
Matsubara F, Shirakura T and Endoh S 2000 *Preprint* cond-mat/0011218
[9] Sadic A and Binder K 1984 *J. Stat. Phys.* **35** 517
[10] Stauffer D 1992 *Physica* A **186** 197
[11] Ito N 1993 *Physica* A **196** 591
[12] Ito N and Ozeki Y 1999 *Int. J. Mod. Phys.* **10** 1495
[13] Huse D A 1989 *Phys. Rev.* B **40** 304
[14] Blundell R E, Humayun K and Bray A J 1992 *J. Phys. A: Math. Gen.* **25** L733

[15] Ozeki Y and Ito N 2001 *Phys. Rev.* B **64** 024416
[16] Ozeki Y, Ogawa K and Ito N 2003 *Phys. Rev.* E **67** 026702
[17] Nakamura T and Endoh S 2002 *J. Phys. Soc. Japan* **71** 2113
[18] Vincent E and Hammann J 1987 *J. Phys. C: Solid State Phys.* **20** 2659
[19] Ogielski A T 1985 *Phys. Rev.* B **32** 7384
[20] Bhatt R N and Young A P 1985 *Phys. Rev. Lett.* **54** 924
[21] Kawashima N and Young A P 1996 *Phys. Rev.* B **53** R484
[22] Palassini M and Caracciolo S 1999 *Phys. Rev. Lett.* **82** 5128
[23] Mari P O and Campbell I A 2002 *Phys. Rev.* B **65** 184409
[24] Gunnarsson K, Svedlindh P, Nordblad P, Lundgren L, Aruga H and Ito A 1991 *Phys. Rev.* B **43** 8199
[25] Morris B W, Colborne S G, Moore M A, Bray A J and Canisius J 1986 *J. Phys. C: Solid State Phys.* **19** 1157
[26] Jain S and Young A P 1986 *J. Phys. C: Solid State Phys.* **19** 3913
[27] Kawamura H and Tanemura M 1987 *Phys. Rev.* B **36** 7177
[28] Kawamura H and Tanemura M 1991 *J. Phys. Soc. Japan* **60** 608
[29] Kawamura H and Li M S 2001 *Phys. Rev. Lett.* **87** 187204
[30] Maucourt J and Grempel D R 1998 *Phys. Rev. Lett.* **80** 770
[31] Akino N and Kosterlitz J M 2002 *Phys. Rev.* B **66** 054536
[32] Lee L W and Young A P 2003 *Phys. Rev. Lett.* **90** 227203
[33] Shirahata T and Nakamura T 2002 *Phys. Rev.* B **65** 024402
[34] Nakamura T 2003 *J. Phys. Soc. Japan* **72** 789